IOPscience iopscience.iop.org

Home Search Collections Journals About Contact us My IOPscience

The formation of a charge layer at the interface of GaMnAs and an organic material

This article has been downloaded from IOPscience. Please scroll down to see the full text article.

2009 EPL 88 46002

(http://iopscience.iop.org/0295-5075/88/4/46002)

View the table of contents for this issue, or go to the journal homepage for more

Download details:
IP Address: 38.107.179.211
The article was downloaded on 16/02/2012 at 04:44

Please note that terms and conditions apply.

A Letters Journal Exploring the Frontiers of Physics

November 2009

EPL, **88** (2009) 46002
doi: 10.1209/0295-5075/88/46002

www.epljournal.org

The formation of a charge layer at the interface of GaMnAs and an organic material

Wenjin Chen[1], Baikui Li[1], Hongtao He[1], Jiannong Wang[1], Hoi Lam Tam[2], Kok Wai Cheah[2], Xiancun Cao[3], Yuqi Wang[3], Guijun Lian[4] and Guangcheng Xiong[4]

[1] *Department of Physics, The Hong Kong University of Science and Technology Clear Water Bay, Kowloon, Hong Kong, China*
[2] *Department of Physics, Hong Kong Baptist University - Kowloon, Hong Kong, China*
[3] *Institute of Solid State Physics, Chinese Academy of Sciences - Hefei, Anhui 230031, China*
[4] *Department of Physics, Peking University - Beijing 100871, China*

received 16 June 2009; accepted in final form 8 November 2009
published online 3 December 2009

PACS 68.35.-p – Solid surfaces and solid-solid interfaces: structure and energetics
PACS 73.40.-c – Electronic transport in interface structures
PACS 79.60.-i – Photoemission and photoelectron spectra

Abstract – The interface formed between the ferromagnetic semiconductor GaMnAs and the organic semiconductor N,N'-diphenyl-N,N'-bis(1-naphthyl)(1,1′-biphenyl)-4,4′-diamine (NPB) was investigated using current transport measurement and ultraviolet photoemission spectroscopy (UPS). The hole injection barrier at a GaMnAs and NPB interface was measured as 0.77 eV by modelling the measured current density-voltage (J-V) characteristics in a GaMnAs/NPB/Al structured device. The vacuum level shift at a GaMnAs/NPB interface was deduced to be 0.54 eV, indicating that a dipole layer exists at the interface. A UPS study gave a vacuum level shift of 0.53 eV and a band offset between the GaMnAs valence band and the highest occupied molecular orbital of NPB of 0.79 eV, in good agreement with the results of J-V measurements. We attribute the vacuum level shift to charge transfer across the interface.

Copyright © EPLA, 2009

Introduction. – Organic semiconductors have been investigated intensively for the past few decades due to their applications in display technology, such as organic light-emitting diodes [1] and organic thin-film transistors [2]. In recent years, because of the weaker spin-orbit coupling and hyperfine interaction, and the longer spin lifetime and spin diffusion length in small molecular organic materials than in inorganic materials, these materials have attracted increasing attention for their potential in spintronic applications [3]. Experimentally, spin-valve devices based on tris(8-hydroxyquinoline) aluminium (Alq3) luminescent material have been studied and spin diffusion lengths up to hundreds of nanometres at low temperature have been reported [4]. Theoretically, the spin-dependent carrier injection and spin polarization have been calculated for different contact resistances at the metal/organic interface [5]. In order to inject spin-polarized carriers into the organic semiconductor, carriers in the electrode must be highly spin-polarized. Ferromagnetic metals (such as Co [3,6,7] and NiFe [6]) and semimetals (such as lanthanum strontium manganese oxide [3,7,8]) have been used in previous studies. For this purpose, the ferromagnetic semiconductor GaMnAs is a potential candidate for the spin-polarized carrier injection electrode. Ferromagnetic GaMnAs has very high spin polarization for holes in the valence band at temperatures below the Curie temperature [9]. In addition, GaMnAs may provide a better conductivity match at the electrode/organic interface in comparison with ferromagnetic metals and this in turn may lead to higher spin injection efficiency [10]. However, there is a lack of investigations on the interface properties between GaMnAs and organic materials. In this paper, we have investigated the interface formed between GaMnAs and N,N'-diphenyl-N,N'-bis(1-naphthyl)(1,1′-biphenyl)-4,4′-diamine (NPB), a prototypical organic hole transporting material. Hole-only devices with a GaMnAs/NPB/Al sandwiched structure were fabricated. Current transport measurements combined with simulation and ultraviolet photoemission spectroscopy (UPS) were used to study the GaMnAs/NPB

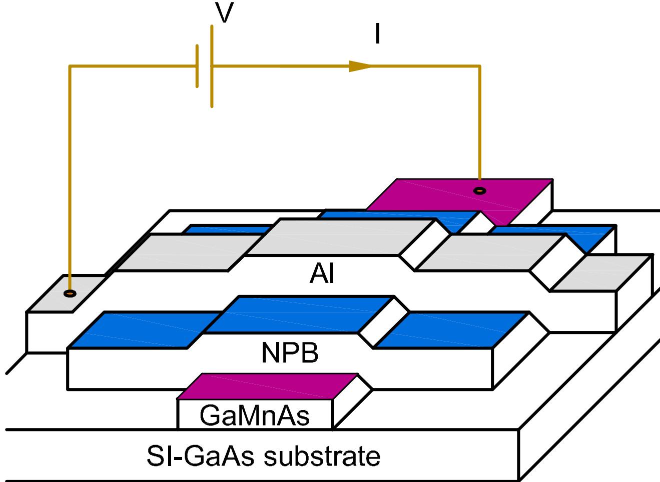

Fig. 1: (Color online) A schematic device structure for J-V measurements. GaMnAs is the anode and Al is the cathode.

interface and to demonstrate that GaMnAs is an effective hole injector in NPB-based organic devices.

Experiments. – Ferromagnetic GaMnAs thin films with a nominal Mn concentration of 5% and a thickness of 20 nm were grown at 250 °C in a Riber 32 MBE system on (001) semi-insulating GaAs (Si-GaAs) substrates [11]. Post-growth annealing was performed in a nitrogen atmosphere at 260 °C for 1 hour to enhance the hole concentration and the ferromagnetism in GaMnAs [12,13]. The Curie temperature of the annealed GaMnAs was 103 K.

The device structure for current-voltage (J-V) measurements is schematically shown in fig. 1. The GaMnAs thin films were patterned into stripes by a standard photolithography process. NPB films of 70 nm and Al films of 60 nm were thermally evaporated onto the patterned substrates using shadow masks in an Edwards Auto 306 system. The device active area was $\sim$400 μm $\times$ 500 μm. After deposition, the devices were transferred into a vacuum chamber where J-V characteristics were measured at room temperature using a HP4155A semiconductor parameter analyzer.

The UPS was performed on a clean GaMnAs surface and NPB thin films of 0.5 nm, 2 nm and 7 nm thickness deposited on GaMnAs. After deposition, the NPB-on-GaMnAs samples were transferred from the Edwards Auto 306 to a UPS measurement chamber immediately, with an air exposure time less than 2 minutes. The light source for the UPS was He I with a photon energy of 21.22 eV. The resolution ($\pm$80 meV) and the position of the Fermi energy E_F in a UPS spectrum were determined from thick, freshly deposited Au films. To distinguish between the secondary electron cut-offs from the sample and detector, a bias of -7.54 V was applied to the sample during the measurement.

In both the J-V and UPS experiments, the GaMnAs samples were etched in diluted HCl solution prior to NPB deposition and for direct UPS measurement. The treatment produces a Ga-Cl terminated surface [14] which is stable in air for at least 1 hour, long enough for the sample transfer [15].

Numerical model. – Numerical simulations of the J-V curves have been carried out to extract the hole injection barrier between the GaMnAs and NPB interface. The theoretical models used include the injection limited current (ILC) model [16–19], and the space charge limited current (SCLC) model [20,21].

In the injection limited current model, the current continuity equation, Poisson's equation, and the drift-diffusion equation are used to describe the charge transport in a GaMnAs/NPB/Al device. Although the electron mobility of NPB can be of the same order of magnitude as the hole mobility [22], the electron injection barrier at the cathode interface (Al/NPB) is as high as 1.75 eV, which is too large for effective electron injection via the Al/NPB interface within the bias range studied [23]. As a result, the device current is conducted almost solely by holes injected from the GaMnAs anode. At the anode interface (GaMnAs/NPB), thermionic emission, interface recombination, and tunnelling injection are all considered to contribute to the total injection current. Neglecting electron-hole recombination, the hole current density is conserved inside the NPB layer:

$$\frac{\mathrm{d}J_p(x)}{\mathrm{d}x} = 0, \tag{1}$$

where $J_p(x)$ is the hole current density inside the NPB layer, x is the position inside NPB starting from the GaMnAs/NPB interface. Neglecting the electron density inside NPB, Poisson's equation is simplified to

$$-\frac{\mathrm{d}^2 V(x)}{\mathrm{d}x^2} = \frac{q}{\varepsilon_r \varepsilon_0} p(x) \tag{2}$$

where $V(x)$ is the electrostatic potential in the NPB layer, $p(x)$ is the hole density, ε_0 is the vacuum permittivity, ε_r is the dielectric constant of NPB normally taken as 3.0 [24], and q is the electron charge. The boundary condition for Poisson's equation is [17]

$$V_a - V_{bi} = \int_0^L E(x)\mathrm{d}x, \tag{3}$$

where V_{bi} is the built-in potential in the NPB layer, and V_a is the applied voltage on the device, L is the thickness of the NPB layer, and $E(x)$ is the electric field within the NPB layer. For a device with the vacuum level aligned, the built-in potential is just the difference between the work function of the two electrodes. However, the vacuum level alignment rule does not generally apply at organic/metal [25–32] and organic/inorganic semiconductor [33–35] interfaces. Taking the vacuum level shift into account, the built-in potential in the device is expressed as

$$V_{bi} = (W_1 - \Delta_1) - (W_2 - \Delta_2)\,, \tag{4}$$

where W_1 and W_2 are the work functions of GaMnAs and Al, respectively, and Δ_1 and Δ_2 are the vacuum level shifts at the GaMnAs/NPB interface and NPB/Al interface, respectively. The work function of Al, W_2, is 4.22 eV and the vacuum level shift at the NPB/Al interface, Δ_2, is 0.45 eV [23]. The ionization energy of GaMnAs, I_{GaMnAs}, is 5.27 eV, after taking into account the broadening of the Mn impurity band and merging it with the GaMnAs valence band [36]. The Fermi energy of metallic GaMnAs is assumed to be aligned with the valence band edge at high doping level. That is, the work function of GaMnAs, W_1, is taken as 5.27 eV. The vacuum level shift at the GaMnAs/NPB interface is unknown prior to the simulation, however it is related to the hole injection barrier ϕ_b (at zero bias) by

$$\Delta_1 = I_{GaMnAs} + \phi_b - I_{NPB}, \tag{5}$$

where I_{GaMnAs} and I_{NPB} are the ionization energies of GaMnAs and NPB, respectively. The ionization energy of NPB was reported to be in the range of 5.4–5.6 eV [33,37,38]. In our simulation, $I_{NPB} = 5.5$ eV is used. The zero-bias hole injection barrier, ϕ_b, is the fitting parameter in our simulation.

The total current density within NPB is composed of both drift and diffusion components [17]:

$$J_p(x) = q\mu_p(E)\left(-p(x)\frac{\mathrm{d}V(x)}{\mathrm{d}x} - \frac{k_BT}{q}\frac{\mathrm{d}p(x)}{\mathrm{d}x}\right), \tag{6}$$

where k_B is Boltzmann's constant, T is the temperature, and $\mu_p(E)$ is the electric field E-dependent hole mobility of NPB. Based on the hopping transport mechanism for organic materials, the field-dependent mobility is of the Poole-Frenkel form [39,40]:

$$\mu(E) = \mu_0 \exp\left(\sqrt{\frac{E}{E_0}}\right), \tag{7}$$

where μ_0 is the zero-field hole mobility and E_0 is a parameter related to material disorder. The hole mobility was reported to be $3.0–6.0 \times 10^{-4}\,\mathrm{cm^2/V\,s}$ [22,24,41], depending on the local electric field using time-of-flight measurements. In our simulation, we choose $\mu_0 = 3.0 \times 10^{-4}\,\mathrm{cm^2/V\,s}$ [22] and $E_0 = 3.90 \times 10^5$ V/cm [42].

The boundary condition for the total current density J_p consists of the thermionic emission current density J_{th}, the interface recombination current density J_{re}, and the Fowler-Nordheim tunnelling current density J_{tu}, *i.e.* [17–19]

$$J_p = J_{th} - J_{re} + J_{tu}. \tag{8}$$

The thermionic emission current density is given as [17]

$$J_{th} = A^*T^2 \exp\left(-\frac{q\phi_b^*}{k_BT}\right), \tag{9}$$

where A^* is Richardson's constant. A^* of $1.2 \times 10^5\,\mathrm{mA/cm^2\,K^2}$ is used [17]. ϕ_b^* is the effective injection barrier at the GaMnAs/NPB interface. When the lowering of the interface barrier due to the image force is taken into account, it is expressed as

$$\phi_b^* = \phi_b - \sqrt{\frac{qE(0)}{4\pi\varepsilon_0\varepsilon_r}}, \tag{10}$$

where $E(0)$ is the electric field at the boundary and ϕ_b is the injection barrier under zero-bias conditions. In the simulation, $E(0)$ and ϕ_b^* are calculated self-consistently. The interface recombination current density is proportional to the hole density [17]:

$$J_{re} = p_b\nu_{rp}, \tag{11}$$

where p_b is the hole density at the GaMnAs and NPB interface and ν_{rp} is a kinetic coefficient at the interface given by $\nu_{rp} = A^*T^2/p_0$ with p_0 being the effective hole density of states in NPB's highest occupied molecular orbital (HOMO). Considering every single molecule as a state, the density of states in the HOMO can be approximated as $p_0 = d_M^{-3} \approx 10^{21}\,\mathrm{cm^{-3}}$, where d_M is the dimension of the NPB molecule [43]. The tunnelling current density is of the Fowler-Nordheim form [44]:

$$J_{tu} = \left(\frac{q^2E^2(0)}{8\pi h\phi_b}\right) \exp\left(-\frac{8\pi\sqrt{2qm_p^*\phi_b^3}}{3hE(0)}\right), \tag{12}$$

where h is Planck's constant, m_p^* is the hole effective mass. Here, $m^* = 9.1 \times 10^{-31}$ kg is used [17].

In the space charge limited current model, the current continuity equation, Poisson's equation and the drift-diffusion equation are the same as those in the injection limited current model. However, with an Ohmic contact, the boundary condition for the current density (*i.e.* eqs. (8)–(12)) is replaced by [21]

$$p(0) = p_0, \tag{13}$$

where $p(0)$ is the hole carrier density at the GaMnAs/NPB interface, and p_0 is the effective hole density of states in NPB HOMO.

Results and discussion. – The forward biased J-V characteristic of a typical GaMnAs/NPB/Al device measured at room temperature with GaMnAs as the anode is shown in fig. 2 (open circles) on a semi-logarithmic scale. The blue solid line and red dash–double-dotted line in the figure are the fitting curves calculated according to the injection limited current model with 0.77 eV hole injection barrier and the space charge limited current model, respectively. In addition, three injection current components in the injection limited model are also shown with the blue dash-dotted line being the thermionic emission component, the green dashed line being the interface recombination component, and the red dotted line being the tunnelling injection component.

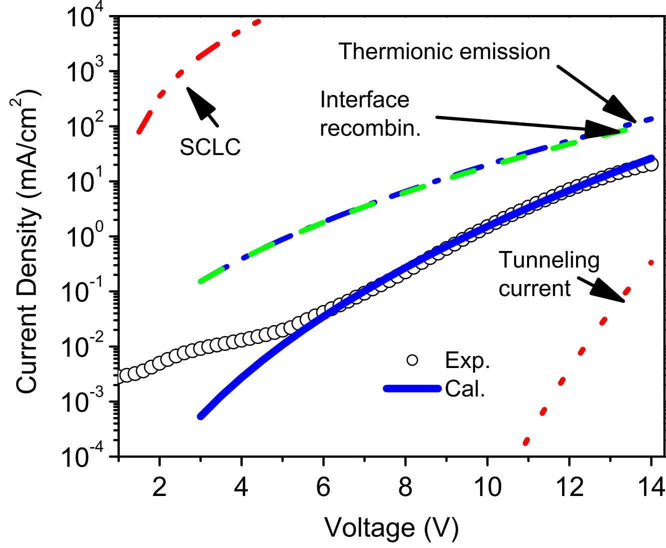

Fig. 2: (Color online) The experimental room temperature J-V curve measured from a typical GaMnAs/NPB/Al device (black open circles) is shown together with the calculated J-V curve using $\phi_b = 0.77$ eV (blue solid line). The calculated thermionic emission current component (blue dash-dotted line), the interface recombination current component (green dashed line), and the tunneling current component (red dotted line) are shown for comparison. The calculated space charge limited current density (red dash–double-dotted line) is also shown as an upper limit.

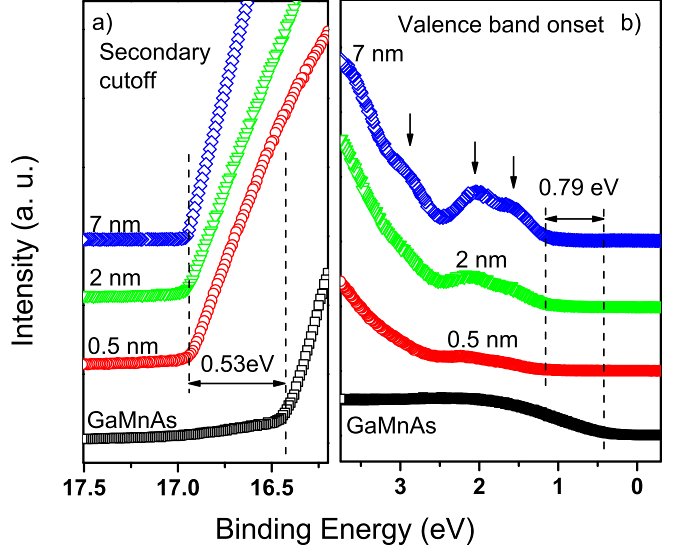

Fig. 3: (Color online) Ultraviolet photoemission spectra (a) near the secondary cut-off and (b) near valence band edge of GaMnAs and NPB on GaMnAs with different NPB film thicknesses as indicated. The spectra are offset for clarity.

It is clear that the current transport in the GaMnAs/NPB/Al device is limited by interface injection as the measured current density is much less than that predicted by the space charge limited current model. The tunnelling current is several orders of magnitude lower than the total current in the measurement voltage range. This means that thermionic emission injection is predominant at room temperature up to 14 V in the GaMnAs/NPB/Al device. However, the strong interface recombination current results in the total current being much less than the thermionic emission current. The discrepancy between the measured and calculated J-V curve in the lower voltage range (0 to 6 V) is possibly due to Ohmic conduction before effective injection starts [18].

From the 0.77 eV hole injection barrier used in the J-V curve fitting, the vacuum level shift at the GaMnAs/NPB interface is deduced from eq. (5) to be 0.54 eV, indicating that a dipole layer exists across the GaMnAs/NPB interface. The possible origin of the dipole is discussed later.

UPS spectra for GaMnAs and NPB samples near the secondary cut-off and valence band edge are shown in figs. 3(a) and (b), respectively. The lowest spectrum (black open squares) is from the clean GaMnAs surface, and the spectra above are from NPB on GaMnAs with NPB film thicknesses of 0.5 nm (red open circles), 2 nm (green open triangles), and 7 nm (blue open diamonds). As can be seen, upon deposition of 0.5 nm of NPB, the UPS spectrum has changed dramatically in comparison with that from clean GaMnAs, indicating effective surface coverage of NPB on GaMnAs. For NPB on GaMnAs, both the spectra onset and the secondary cut-off positions are shifted towards higher binding energies independent of the NPB layer thickness. As the NPB layer thickness increases, the new features at 1.60 eV, 2.10 eV and 2.90 eV (see arrows in fig. 3(b) become more and more clear, indicating that these features are characteristics of NPB molecular levels. The fact that the features observed in this study are the same as those reported previously [33,37] for NPB films deposited on other substrates suggests that the NPB layer does not undergo noticeable dissociation on the HCl-passivated GaMnAs surface. It is also noticed that no observable shifts of these NPB associated features occur with increasing NPB film thickness, implying that band bending in thin NPB film is negligible due to its low intrinsic carrier density.

In UPS studies, the ionization energy (I) in semiconductors, defined as the energy separation between the valence band edge (or HOMO edge) and the vacuum level, can be determined by subtracting the photon energy ($h\nu$) from the spectrum width. Denoting the secondary cut-off energy as E_{sec} and the valence band onset energy as E_{ons}, the ionization energy I is then given as $h\nu - (E_{ons} - E_{sec})$. As a result, the ionization energy of GaMnAs is deduced to be 5.24 eV from the spectrum in figs. 3(a) and (b), which is in good agreement with the value of 5.27 eV reported elsewhere [36]. The NPB ionization energy of 5.50 eV is obtained in the same way, which is also in good agreement with the reported value of 5.4–5.6 eV [33,37,38].

The valence band onset of the GaMnAs UPS spectrum in fig. 3(b) is 0.43 eV. This implies that the Fermi energy

at the GaMnAs surface is within the band gap. For a GaMnAs thin film with a Mn concentration of 5%, the Fermi energy lies within the valence band in the bulk region, the energy band is therefore bent downwards at the surface of GaMnAs due to surface depletion effects. The HOMO onset of NPB on GaMnAs is shifted to 1.22 eV (see fig. 3(b)). Consequently, the band offset between the GaMnAs valence band edge and the NPB HOMO at the interface is determined to be 0.79 eV as indicated in fig. 3(b).

Furthermore, the work function can also be determined from the UPS spectrum by subtracting the photon energy $h\nu$ from the secondary cut-off energy E_{sec}. As a result, the GaMnAs work function of 4.81 eV and NPB work function of 4.28 eV are obtained from the spectra in fig. 3(a). The work function difference between NPB and GaMnAs reflects a sudden shift of vacuum level across the GaMnAs/NPB interface indicating the formation of an interface dipole. This shift is equal to 0.53 eV, almost the same as that obtained in the J-V study discussed above. As shown in fig. 3(a), this shift does not change with NPB film thickness.

Based on the above analysis, the band diagram of the GaMnAs/NPB structure is summarized in fig. 4. The sign of the interface dipole is marked in red. The band bending on the GaMnAs side and the lowest unoccupied molecular orbital (LUMO) of NPB are shown schematically. It has been generally observed that the vacuum level alignment rule does not hold at organic/metal [25–32] and organic/inorganic semiconductor interfaces [33–35], suggesting the formation of a dipole layer across the interface. For non-polar molecular organics, the possible origins of the dipole layer include charge transfer across the interface and chemical reactions [45]. Chemical reaction typically takes place in structures where metal is deposited on the organic layer, possibly due to the high reactivity of the vaporized hot metal atoms or the diffusion of metal atoms into the organic layer [4,46]. Organic-on-metal structures are usually more stable, except for some active chemical reactions, *e.g.* Alq3-metal complexes [47,48]. In this study, the GaMnAs substrate is etched in dilute HCl solution to produce a stable surface prior to NPB deposition, the chemical reaction is therefore unlikely to occur at the GaMnAs/NPB interface. On the other hand, direct charge transfer is expected only at interfaces formed between strong acceptor organics and low work function metals, or between strong donor organics and high work function metals [28,29]. The measured charge injection barrier of 0.79 eV implies that direct transfer of holes from the GaMnAs valence band to NPB HOMO is unlikely to happen in our structure. In addition to direct charge transfer, however, metal-induced gap states have recently been proposed to explain metal/organic interface dipole formation [27,30–32]. These gap states can be either donor-like (close to the valence band) or acceptor-like (close to the conduction band). Charge neutrality is then defined as the point separating the donor-like and acceptor-like levels. The charge neutrality level tends to align with the Fermi energy of the electrode as a result of charge transfer between the electrode and the induced gap states, forming an interface dipole. Based on this mechanism, GaMnAs with a very high hole concentration ($\sim 10^{20}/\mathrm{cm}^3$) induces gap states at the GaMnAs/NPB interface. As the charge neutrality level of NPB (4.1–4.2 eV [30–32]) is much smaller than the work function of GaMnAs (4.81 eV), it is believed that charge transfer occurs between GaMnAs and NPB interface gap states, and an interface dipole pointing from NPB to GaMnAs is formed, as shown in fig. 4.

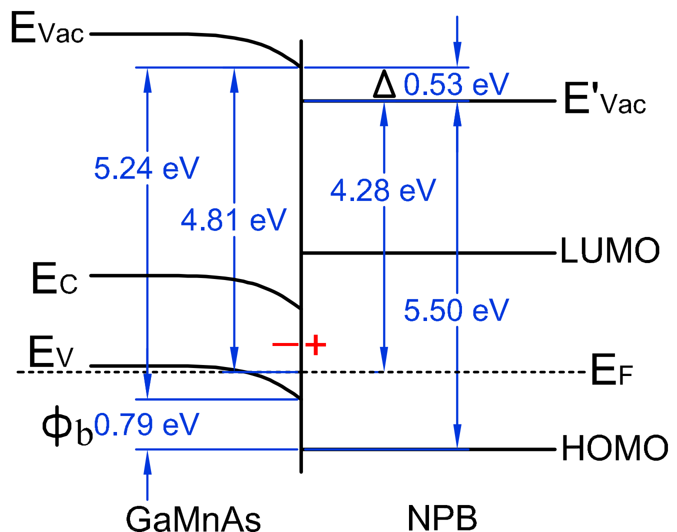

Fig. 4: (Color online) The energy band alignment diagram of the GaMnAs/NPB interface deduced from UPS analysis. E_v and E_c are the valence and conduction band edge of GaMnAs, respectively. E_{Vac} and E'_{Vac} are the vacuum level on the GaMnAs side and NPB side, respectively. E_F is the Fermi energy, Δ is the vacuum level shift at the GaMnAs and NPB interface, and ϕ_b is the band edge offset between the GaMnAs valence band edge and NPB HOMO. The red marker indicates the charges forming the interface dipole.

Conclusions. – An interface formed between GaMnAs and NPB is studied by J-V and UPS measurements. The hole injection barrier and the vacuum level shift at the GaMnAs and NPB interfaces is estimated to be 0.77 eV and 0.54 eV, respectively, by fitting the measured room temperature J-V characteristics. The band offset between the GaMnAs valence band edge and NPB HOMO and the vacuum level shift at the interface are measured to be 0.79 eV and 0.53 eV, respectively, in a UPS study. The barrier height (or band offset) and the vacuum level shift obtained in the current transport study and UPS analysis are in good agreement. The formation of an interface dipole is probably due to charge transfer between GaMnAs and NPB interface gap states. This study indicates that measuring and fitting the J-V curve with known material parameters provides us with an alternative way of estimating band alignment at an inorganic/organic interface.

∗∗∗

The authors are grateful for the financial support from the Research Grant Council of Hong Kong SAR government via grant No. N_HKUST611/05.

REFERENCES

[1] Tang C. W. and Vanslyke S. A., *Appl. Phys. Lett.*, **51** (1987) 913.
[2] Dodabalapur A., Torsi L. and Katz H. E., *Science*, **268** (1995) 270.
[3] Naber W. J. M., Faez S. and Van De Wiel W. G., *J. Phys. D: Appl. Phys.*, **40** (2007) R205.
[4] Xiong Z. H., Wu D., Valy Vardeny Z. and Shi J., *Nature*, **427** (2004) 821.
[5] Yunus M., Ruden P. P. and Smith D. L., *J. Appl. Phys.*, **103** (2008) 103714.
[6] Santos T. S., Lee J. S., Migdal P., Lekshmi I. C., Satpati B. and Moodera J. S., *Phys. Rev. Lett.*, **98** (2007) 016601.
[7] Wang F. J., Yang C. G., Valy Vardeny Z. and Li X. G., *Phys. Rev. B*, **75** (2007) 245324.
[8] Dediu V., Murgia M., Matacotta F. C., Taliani C. and Barbanera S., *Solid State Commun.*, **122** (2002) 181.
[9] Sapega V. F., Moreno M., Ramsteiner M., Däweritz L. and Ploog K. H., *Phys. Rev. Lett.*, **94** (2005) 137401.
[10] Ohno Y., Young D. K., Beschoten B., Matsukura F., Ohno H. and Awschalom D. D., *Nature*, **402** (1999) 790.
[11] Ji C. J., Cao X. C., Han Q. F., Qiu K., Zhong F., Li X. H., He H. T., Wang J. N. and Wang Y. Q., *Appl. Phys. Lett.*, **90** (2007) 232501.
[12] Hayashi T., Hashimoto Y., Katsumoto S. and Iye Y., *Appl. Phys. Lett.*, **78** (2001) 1691.
[13] Ji C. J., He H. T., Cao X. C., Qiu K., Zhong F., Li X. H., Han Q. F., Xu F. Q., Wang J. N. and Wang Y. Q., *EPL*, **78** (2007) 57006.
[14] Kang M. G., Sa S. H., Park H. H., Suh K. S. and Oh K. H., *Thin Solid Films*, **308-309** (1997) 634.
[15] Lu Z. H., Chatenoud F., Dion M. M., Graham M. J., Ruda H. E., Koutzarov I., Liu Q., Mitchell C. E. J., Hill I. G. and Mclean A. B., *Appl. Phys. Lett.*, **67** (1995) 670.
[16] Parker I. D., *J. Appl. Phys.*, **75** (1994) 1656.
[17] Davids P. S., Campbell I. H. and Smith D. L., *J. Appl. Phys.*, **82** (1997) 6319.
[18] Campbell A. J., Bradley D. D. C., Laubender J. and Sokolowski M., *J. Appl. Phys.*, **86** (1999) 5004.
[19] Brütting W., Berleb S. and Mückl A. G., *Org. Electron.*, **2** (2001) 1.
[20] Blom P. W. M., De Jong M. J. M. and Vleggaar J. J. M., *Appl. Phys. Lett.*, **68** (1996) 3308.
[21] Blom P. W. M., Jong M. J. M. and Van Munster M. G., *Phys. Rev. B*, **55** (1997) R656.
[22] Tse S. C., Kwok K. C. and So S. K., *Appl. Phys. Lett.*, **89** (2006) 262102.
[23] Xie Z. T., Ding B. F., Gao X. D., You Y. T., Sun Z. Y., Zhang W. H., Ding X. M. and Hou X. Y., *J. Appl. Phys.*, **105** (2009) 106105.
[24] Schwartz G., Ke T. H., Wu C. C., Walzer K. and Leo K., *Appl. Phys. Lett.*, **93** (2008) 073304.
[25] Bardeen J., *Phys. Rev.*, **71** (1947) 717.
[26] Cowley A. M. and Sze S. M., *J. Appl. Phys.*, **36** (1965) 3212.
[27] Mönch W., *Phys. Rev. Lett.*, **58** (1987) 1260.
[28] Hill I. G., Rajagopal A., Kahn A. and Hu Y., *Appl. Phys. Lett.*, **73** (1998) 662.
[29] Ishii H., Sugiyama K., Ito E. and Seki K., *Adv. Mater.*, **11** (1999) 605.
[30] Vázquez H., Gao W., Flores F. and Kahn A., *Phys. Rev. B*, **71** (2005) 041306(R).
[31] Vázquez H., Flores F. and Kahn A., *Org. Electron.*, **8** (2007) 241.
[32] Helander M. G., Wang Z. B., Qiu J. and Lu Z. H., *Appl. Phys. Lett.*, **93** (2008) 193310.
[33] Chassé T., Wu C.-I., Hill I. G. and Kahn A.,, *J. Appl. Phys.*, **85** (1999) 6589.
[34] Hirose Y., Chen W., Haskal E. I., Forrest S. R. and Kahn A., *Appl. Phys. Lett.*, **64** (1994) 3482.
[35] Kampen T. U., Gavrila G., Mendez H., Zahn D. R. T., Vearey-Roberts A. R., Evans D. A., Wells J., Mcgovern I. and Braun W., *J. Phys.: Condens. Matter*, **15** (2003) S2679.
[36] Jungwirth T., Sinova J., Macdonald A. H., Gallagher B. L., Novák V., Edmonds K. W., Rushforth A. W., Campion R. P., Foxon C. T., Eaves L., Olejník E., Mašek J., Eric Yang S.-R., Wunderlich J., Gould C., Molenkamp L. W., Dietl T. and Ohno H., *Phys. Rev. B*, **76** (2007) 125206.
[37] Le Q. T., Nüesch F., Rothberg L. J., Forsythe E. W. and Gao Y., *Appl. Phys. Lett.*, **75** (1999) 1357.
[38] Kahn A., Koch N. and Gao W., *J. Polym. Sci. Part B: Polym. Phys.*, **41** (2003) 2529.
[39] Bässler H., *Phys. Status Solidi (b)*, **175** (1993) 15.
[40] Murgatroyd P. N., *J. Phys. D: Appl. Phys.*, **3** (1970) 151.
[41] Forsythe E. W., Abkowitz M. A. and Gao Y., *J. Phys. Chem. B*, **104** (2000) 3948.
[42] Tsang S. W., Lu Z. H. and Tao Y., *Appl. Phys. Lett.*, **90** (2007) 132115.
[43] Staudigel J., Stößel M., Steuber F. and Simmerer J., *J. Appl. Phys.*, **86** (1999) 3895.
[44] Fowler R. H. and Nordheim L., *Proc. R. Soc. London, Ser. A*, **119** (1928) 173.
[45] Hoelzel J., Schulte F. K. and Wagner H., *Solid State Surface Physics* (Springer, Berlin) 1979.
[46] Tarlov M. J., *Langmuir*, **8** (1992) 80.
[47] Choong V.-E., Mason M. G., Tang C. W. and Gao Y., *Appl. Phys. Lett.*, **72** (1998) 2689.
[48] Curioni A. and Andreoni W., *J. Am. Chem. Soc.*, **121** (1999) 8216.